LABORATOIRE EUROPEEN POUR LA PHYSIQUE DES PARTICULES (CERN)

CERN-EP/98-145
16-Sept-1998

# Searches for the Neutral Higgs Bosons of the MSSM in $e^+e^-$ Collisions at Centre-of-mass Energies of 181–184 GeV

The ALEPH Collaboration*)

**Abstract**

The data collected by ALEPH at LEP at centre-of-mass energies ranging from 181 to 184 GeV, corresponding to an integrated luminosity of 57 $\mathrm{pb}^{-1}$, are analysed to search for pair-produced neutral Higgs bosons h and A, in the $\mathrm{b\bar{b}b\bar{b}}$ and $\tau^+\tau^-\mathrm{b\bar{b}}$ final states. Two events are found in the data with 2.5 expected from standard model processes. When combined with the lower energy data collected by ALEPH and with earlier reported searches for associated hZ production, these analyses are interpreted in the context of the minimal supersymmetric extension of the standard model (MSSM). For standard choices of MSSM parameter sets, this combination results in 95% C.L. exclusion lower limits of 72.2 and 76.1 GeV/$c^2$ for $m_\mathrm{h}$ and $m_\mathrm{A}$, irrespective of $\tan\beta$. A scan of the MSSM parameter space is performed in which the model parameters are varied over wide ranges. For low values of $\tan\beta$, *i.e.*, for $1 < \tan\beta \lesssim 2$, the limit on $m_\mathrm{h}$ of $\sim 88$ GeV/$c^2$ is shown to be robust, being satisfied in essentially all of the physically allowed domain.

*To appear in Physics Letters B*

*) See next pages for the list of authors

# The ALEPH Collaboration

R. Barate, D. Buskulic, D. Decamp, P. Ghez, C. Goy, S. Jezequel, J.-P. Lees, A. Lucotte, F. Martin, E. Merle, M.-N. Minard, J.-Y. Nief, P. Perrodo, B. Pietrzyk

*Laboratoire de Physique des Particules (LAPP), IN$^2$P$^3$-CNRS, F-74019 Annecy-le-Vieux Cedex, France*

R. Alemany, M.P. Casado, M. Chmeissani, J.M. Crespo, M. Delfino, E. Fernandez, M. Fernandez-Bosman, Ll. Garrido,[15] E. Graugès, A. Juste, M. Martinez, G. Merino, R. Miquel, Ll.M. Mir, P. Morawitz, A. Pacheco, I.C. Park, A. Pascual, I. Riu, F. Sanchez

*Institut de Física d'Altes Energies, Universitat Autònoma de Barcelona, 08193 Bellaterra (Barcelona), E-Spain*[7]

A. Colaleo, D. Creanza, M. de Palma, G. Gelao, G. Iaselli, G. Maggi, M. Maggi, S. Nuzzo, A. Ranieri, G. Raso, F. Ruggieri, G. Selvaggi, L. Silvestris, P. Tempesta, A. Tricomi,[3] G. Zito

*Dipartimento di Fisica, INFN Sezione di Bari, I-70126 Bari, Italy*

X. Huang, J. Lin, Q. Ouyang, T. Wang, Y. Xie, R. Xu, S. Xue, J. Zhang, L. Zhang, W. Zhao

*Institute of High-Energy Physics, Academia Sinica, Beijing, The People's Republic of China*[8]

D. Abbaneo, U. Becker,[22] G. Boix,[24] M. Cattaneo, F. Cerutti, V. Ciulli, G. Dissertori, H. Drevermann, R.W. Forty, M. Frank, F. Gianotti, R. Hagelberg, A.W. Halley, J.B. Hansen, J. Harvey, P. Janot, B. Jost, I. Lehraus, O. Leroy, P. Maley, P. Mato, A. Minten, L. Moneta,[20] A. Moutoussi, F. Ranjard, L. Rolandi, D. Rousseau, D. Schlatter, M. Schmitt,[1] O. Schneider, W. Tejessy, F. Teubert, I.R. Tomalin, E. Tournefier, M. Vreeswijk, H. Wachsmuth

*European Laboratory for Particle Physics (CERN), CH-1211 Geneva 23, Switzerland*

Z. Ajaltouni, F. Badaud G. Chazelle, O. Deschamps, S. Dessagne, A. Falvard, C. Ferdi, P. Gay, C. Guicheney, P. Henrard, J. Jousset, B. Michel, S. Monteil, J-C. Montret, D. Pallin, P. Perret, F. Podlyski

*Laboratoire de Physique Corpusculaire, Université Blaise Pascal, IN$^2$P$^3$-CNRS, Clermont-Ferrand, F-63177 Aubière, France*

J.D. Hansen, J.R. Hansen, P.H. Hansen, B.S. Nilsson, B. Rensch, A. Wäänänen

*Niels Bohr Institute, 2100 Copenhagen, DK-Denmark*[9]

G. Daskalakis, A. Kyriakis, C. Markou, E. Simopoulou, A. Vayaki

*Nuclear Research Center Demokritos (NRCD), GR-15310 Attiki, Greece*

A. Blondel, J.-C. Brient, F. Machefert, A. Rougé, M. Rumpf, R. Tanaka, A. Valassi,[6] H. Videau

*Laboratoire de Physique Nucléaire et des Hautes Energies, Ecole Polytechnique, IN$^2$P$^3$-CNRS, F-91128 Palaiseau Cedex, France*

E. Focardi, G. Parrini, K. Zachariadou

*Dipartimento di Fisica, Università di Firenze, INFN Sezione di Firenze, I-50125 Firenze, Italy*

R. Cavanaugh, M. Corden, C. Georgiopoulos, T. Huehn, D.E. Jaffe

*Supercomputer Computations Research Institute, Florida State University, Tallahassee, FL 32306-4052, USA* [13,14]

A. Antonelli, G. Bencivenni, G. Bologna,[4] F. Bossi, P. Campana, G. Capon, V. Chiarella, P. Laurelli, G. Mannocchi,[5] F. Murtas, G.P. Murtas, L. Passalacqua, M. Pepe-Altarelli[12]

*Laboratori Nazionali dell'INFN (LNF-INFN), I-00044 Frascati, Italy*

M. Chalmers, L. Curtis, J.G. Lynch, P. Negus, V. O'Shea, C. Raine, J.M. Scarr, P. Teixeira-Dias, A.S. Thompson, E. Thomson, J.J. Ward

*Department of Physics and Astronomy, University of Glasgow, Glasgow G12 8QQ,United Kingdom*[10]

O. Buchmüller, S. Dhamotharan, C. Geweniger, P. Hanke, G. Hansper, V. Hepp, E.E. Kluge, A. Putzer, J. Sommer, K. Tittel, S. Werner, M. Wunsch

*Institut für Hochenergiephysik, Universität Heidelberg, D-69120 Heidelberg, Germany*[16]

R. Beuselinck, D.M. Binnie, W. Cameron, P.J. Dornan,[12] M. Girone, S. Goodsir, N. Marinelli, E.B. Martin, J. Nash, J.K. Sedgbeer, P. Spagnolo, M.D. Williams

*Department of Physics, Imperial College, London SW7 2BZ, United Kingdom*[10]

V.M. Ghete, P. Girtler, E. Kneringer, D. Kuhn, G. Rudolph

*Institut für Experimentalphysik, Universität Innsbruck, A-6020 Innsbruck, Austria*[18]

A.P. Betteridge, C.K. Bowdery, P.G. Buck, P. Colrain, G. Crawford, G. Ellis, A.J. Finch, F. Foster, G. Hughes, R.W.L. Jones, A.N. Robertson, M.I. Williams

*Department of Physics, University of Lancaster, Lancaster LA1 4YB, United Kingdom*[10]

P. van Gemmeren, I. Giehl, C. Hoffmann, K. Jakobs, K. Kleinknecht, M. Kröcker, H.-A. Nürnberger, G. Quast, B. Renk, E. Rohne, H.-G. Sander, S. Schmeling, C. Zeitnitz, T. Ziegler

*Institut für Physik, Universität Mainz, D-55099 Mainz, Germany*[16]

J.J. Aubert, C. Benchouk, A. Bonissent, J. Carr,[12] P. Coyle, A. Ealet, D. Fouchez, F. Motsch, P. Payre, M. Talby, M. Thulasidas, A. Tilquin

*Centre de Physique des Particules, Faculté des Sciences de Luminy, IN$^2$P$^3$-CNRS, F-13288 Marseille, France*

M. Aleppo, M. Antonelli, F. Ragusa

*Dipartimento di Fisica, Università di Milano e INFN Sezione di Milano, I-20133 Milano, Italy.*

R. Berlich, V. Büscher, H. Dietl, G. Ganis, K. Hüttmann, G. Lütjens, C. Mannert, W. Männer, H.-G. Moser, S. Schael, R. Settles, H. Seywerd, H. Stenzel, W. Wiedenmann, G. Wolf

*Max-Planck-Institut für Physik, Werner-Heisenberg-Institut, D-80805 München, Germany*[16]

J. Boucrot, O. Callot, S. Chen, M. Davier, L. Duflot, J.-F. Grivaz, Ph. Heusse, A. Höcker, A. Jacholkowska, M. Kado, D.W. Kim,[2] F. Le Diberder, J. Lefrançois, L. Serin, J.-J. Veillet, I. Videau,[12] J.-B. de Vivie de Régie, D. Zerwas

*Laboratoire de l'Accélérateur Linéaire, Université de Paris-Sud, IN$^2$P$^3$-CNRS, F-91898 Orsay Cedex, France*

P. Azzurri, G. Bagliesi,[12] S. Bettarini, T. Boccali, C. Bozzi, G. Calderini, R. Dell'Orso, R. Fantechi, I. Ferrante, A. Giassi, A. Gregorio, F. Ligabue, A. Lusiani, P.S. Marrocchesi, A. Messineo, F. Palla, G. Rizzo, G. Sanguinetti, A. Sciabà, G. Sguazzoni, R. Tenchini, C. Vannini, A. Venturi, P.G. Verdini

*Dipartimento di Fisica dell'Università, INFN Sezione di Pisa, e Scuola Normale Superiore, I-56010 Pisa, Italy*

G.A. Blair, J.T. Chambers, J. Coles, G. Cowan, M.G. Green, T. Medcalf, J.A. Strong, J.H. von Wimmersperg-Toeller

*Department of Physics, Royal Holloway & Bedford New College, University of London, Surrey TW20 OEX, United Kingdom*[10]

D.R. Botterill, R.W. Clifft, T.R. Edgecock, P.R. Norton, J.C. Thompson, A.E. Wright

*Particle Physics Dept., Rutherford Appleton Laboratory, Chilton, Didcot, Oxon OX11 OQX, United Kingdom*[10]

B. Bloch-Devaux, P. Colas, B. Fabbro, G. Faïf, E. Lançon,[12] M.-C. Lemaire, E. Locci, P. Perez, H. Przysiezniak, J. Rander, J.-F. Renardy, A. Rosowsky, A. Trabelsi,[23] B. Tuchming, B. Vallage

*CEA, DAPNIA/Service de Physique des Particules, CE-Saclay, F-91191 Gif-sur-Yvette Cedex, France*[17]

S.N. Black, J.H. Dann, H.Y. Kim, N. Konstantinidis, A.M. Litke, M.A. McNeil, G. Taylor

*Institute for Particle Physics, University of California at Santa Cruz, Santa Cruz, CA 95064, USA*[19]

C.N. Booth, S. Cartwright, F. Combley, M.S. Kelly, M. Lehto, L.F. Thompson
*Department of Physics, University of Sheffield, Sheffield S3 7RH, United Kingdom*[10]

K. Affholderbach, A. Böhrer, S. Brandt, J. Foss, C. Grupen, G. Prange, L. Smolik, F. Stephan
*Fachbereich Physik, Universität Siegen, D-57068 Siegen, Germany*[16]

G. Giannini, B. Gobbo
*Dipartimento di Fisica, Università di Trieste e INFN Sezione di Trieste, I-34127 Trieste, Italy*

J. Putz, J. Rothberg, S. Wasserbaech, R.W. Williams
*Experimental Elementary Particle Physics, University of Washington, WA 98195 Seattle, U.S.A.*

S.R. Armstrong, E. Charles, P. Elmer, D.P.S. Ferguson, Y. Gao, S. González, T.C. Greening, O.J. Hayes, H. Hu, S. Jin, G. Mamier, P.A. McNamara III, J.M. Nachtman,[21] J. Nielsen, W. Orejudos, Y.B. Pan, Y. Saadi, I.J. Scott, M. Vogt, J. Walsh, Sau Lan Wu, X. Wu, G. Zobernig
*Department of Physics, University of Wisconsin, Madison, WI 53706, USA*[11]

[1]Now at Harvard University, Cambridge, MA 02138, U.S.A.
[2]Permanent address: Kangnung National University, Kangnung, Korea.
[3]Also at Dipartimento di Fisica, INFN Sezione di Catania, Catania, Italy.
[4]Also Istituto di Fisica Generale, Università di Torino, Torino, Italy.
[5]Also Istituto di Cosmo-Geofisica del C.N.R., Torino, Italy.
[6]Now at LAL, Orsay
[7]Supported by CICYT, Spain.
[8]Supported by the National Science Foundation of China.
[9]Supported by the Danish Natural Science Research Council.
[10]Supported by the UK Particle Physics and Astronomy Research Council.
[11]Supported by the US Department of Energy, grant DE-FG0295-ER40896.
[12]Also at CERN, 1211 Geneva 23,Switzerland.
[13]Supported by the US Department of Energy, contract DE-FG05-92ER40742.
[14]Supported by the US Department of Energy, contract DE-FC05-85ER250000.
[15]Permanent address: Universitat de Barcelona, 08208 Barcelona, Spain.
[16]Supported by the Bundesministerium für Bildung, Wissenschaft, Forschung und Technologie, Germany.
[17]Supported by the Direction des Sciences de la Matière, C.E.A.
[18]Supported by Fonds zur Förderung der wissenschaftlichen Forschung, Austria.
[19]Supported by the US Department of Energy, grant DE-FG03-92ER40689.
[20]Now at University of Geneva, 1211 Geneva 4, Switzerland.
[21]Now at University of California at Los Angeles (UCLA), Los Angeles, CA 90024, U.S.A.
[22]Now at SAP AG, D-69185 Walldorf, Germany
[23]Now at Département de Physique, Faculté des Sciences de Tunis, 1060 Le Belvédère, Tunisia.
[24]Supported by the Commission of the European Communities, contract ERBFMBICT982894.

# 1 Introduction

In the minimal supersymmetric extension of the standard model (MSSM), the Higgs sector consists of five physical states, namely three neutral bosons – two CP-even (h and H), and one CP-odd (A) – and a pair of charged bosons ($H^{\pm}$). At LEP2 energies, the neutral Higgs bosons can be produced via two complementary processes, the Higgs-strahlung process $e^+e^- \to hZ$, with a small contribution from the WW and ZZ fusion processes to the $h\nu\bar{\nu}$ and $he^+e^-$ final states, with a cross section proportional to $\sin^2(\beta-\alpha)$, and the associated production $e^+e^- \to hA$ with a cross section proportional to $\cos^2(\beta-\alpha)$. Here, $\alpha$ is the mixing angle in the CP-even sector, and $\tan\beta$ is the ratio of the vacuum expectation values of the two Higgs doublets.

The Higgs-strahlung process and associated production have already been investigated by ALEPH at centre-of-mass energies from 130 to 172 GeV [1, 2]. Searches for the Higgs-strahlung process at energies around 183 GeV were also reported in Ref. [3]. In all of these searches, the events selected in the data were found to be compatible with expectations from standard model background processes. Similar results have been obtained by the other LEP experiments [4].

This letter presents an update of the associated production search using the 57 $pb^{-1}$ of data collected with the ALEPH detector at LEP at $\sqrt{s}$ from 181 to 184 GeV during 1997. For most MSSM parameter values, the prominent decay modes of h and A are into $b\bar{b}$ ($\sim 90\%$) and $\tau^+\tau^-$ ($\sim 10\%$), leading to the two dominant final states $b\bar{b}b\bar{b}$ and $\tau^+\tau^-b\bar{b}$.

The combination of the searches for these two topologies and for those produced by the Higgs-strahlung process are sufficient to cover the vast majority of the kinematically accessible configurations predicted by the MSSM. This is in particular the case for the benchmark parameter sets suggested in Ref. [5], the so-called minimal and maximal mixing configurations.

However, in some regions of the MSSM parameter space, other decays may open up and/or the usual pattern of couplings and masses may be affected in such a way that the traditional hZ and hA searches are rendered ineffective. An account of these anomalous configurations is given in this letter, the detailed analysis of which can be found in Ref. [6].

This letter is organized as follows. In Section 2, the relevant aspects of the ALEPH detector and the b quark tagging performance are described. Event selections used in the various search channels are presented in Section 3. In Section 4, the results from the analyses presented in this letter are combined with results from the updated hZ search [3], and are interpreted in the context of the benchmark parameter configurations of the MSSM. Finally, a more general interpretation of these results is given in Section 5 where a scan of the parameter space of the MSSM is performed taking into account searches for charged Higgs bosons [7], for invisible Higgs boson decays [8], for supersymmetric particles [9, 10] and various LEP 1 results [11, 12, 13].

## 2 The ALEPH detector

The ALEPH detector and its performance are described in Refs. [14, 15, 16]. The tracking system consists of the silicon vertex detector surrounded by the inner tracking chamber and the time projection chamber. A 1.5 T axial magnetic field delivered by a superconducting solenoidal coil allows a charged particle $1/p_T$ resolution of $(6 \times 10^{-4} \bigoplus 5 \times 10^{-3}/p_T)$ $(\mathrm{GeV}/c)^{-1}$ to be achieved. The three-dimensional impact parameter resolution of charged particle tracks with coordinates in the silicon vertex detector can be parametrized as $(34+70/p)\times(1+1.6\cos^4\theta)$ $\mu$m, with $p$ in GeV/$c$, and is used to identify b quark jets. Charged particle tracks are used in these analyses if they are reconstructed with at least four hits in the time projection chamber and originate from within a cylinder of length 20 cm and radius 2 cm coaxial with the beam and centered at the nominal interaction point. Events with at least eight such *good tracks* accounting for more than 10% of the centre-of-mass energy are referred to as hadronic events.

Electrons are identified by combining the information from the specific ionization measurement in the time projection chamber with information from the lead/proportional chamber electromagnetic calorimeter. The calorimeter has fine readout segmentation and a total thickness of 22 radiation lengths at normal incidence. It provides a relative electromagnetic energy resolution of $0.18/\sqrt{E} + 0.009$ ($E$ in GeV) for isolated electrons and photons.

Muons are identified by a hit pattern characteristic of a penetrating particle in the hadron calorimeter, a 1.2 m thick magnet return yoke instrumented with 23 layers of streamer tubes, and in the two surrounding layers of muon chambers. Together with the electromagnetic calorimeter, the hadron calorimeter also provides a measurement of the energy of charged and neutral hadrons with a relative resolution of $0.85/\sqrt{E}$ ($E$ in GeV).

This information is combined in an energy flow algorithm. When the measurements from the above detectors are supplemented with measurements of energy detected at low polar angles by additional electromagnetic calorimeters principally used for luminosity determination, the total energy, and therefore the missing energy can be measured. The energy flow algorithm gives a measurement of the total energy with a resolution of $(0.6\sqrt{E}+0.6)$ GeV ($E$ in GeV) for hadronic events. The charged and neutral objects reconstructed with this algorithm are called *energy-flow particles* and are used to form jets, with a typical angular resolution of 20 mrad for both polar and azimuthal angles, and a relatively uniform energy resolution over the whole detector acceptance.

Jets originating from b quarks are identified by taking advantage of the lifetime of b hadrons, and of the presence in the jets of high $p_T$ leptons. Algorithms based on track impact parameters [17] and secondary decay vertices [18] are used to detect the presence of long-lived b hadrons, while the identified lepton of highest transverse momentum in the jet (relative to the jet it belongs to) is used to search for semileptonic decays of heavy b hadrons. These quantities are input into a neural network trained to discriminate between jets containing b hadrons (giving a neural network output $\eta$ close to 1) and those originating from light quarks ($\eta \simeq 0$). The neural network is similar in structure and in performance to the one used to analyse the data collected at centre-of-mass energies of 130 to 172 GeV [2].

# 3 Update of the $e^+e^- \to hA$ event selections

As at lower centre-of-mass energies, the search for the hA pair-production process consists of different topological selections addressing the $b\bar{b}b\bar{b}$ and the $\tau^+\tau^-b\bar{b}$ final states. The selections described in Ref. [2] were used again to analyse the data taken in 1997. In the final states with $\tau$'s, however, the two selection algorithms were unified in a selection based on a neural network combination of the existing discriminating variables.

These selections were optimized for hA production with $m_h = m_A = 75$ GeV/$c^2$, close to the actual sensitivity of the experiment for $\cos^2(\beta-\alpha) = 1$. To do so, the expected combined confidence level that would be obtained on average if no signal were present [19] was minimized with respect to (some of) the most relevant selection cuts of the two analyses, namely on

- a variable $\mathcal{F}$, combining the b quark content and the four-jet compatibility in the $b\bar{b}b\bar{b}$ channel;
- the neural network output in the $\tau^+\tau^-b\bar{b}$ final state.

In parallel, the selectivity of the confidence level determined from the $b\bar{b}b\bar{b}$ search was improved with respect to Ref. [2] by including $\mathcal{F}$ in the test statistic, in addition to the sum of the two reconstructed Higgs boson masses (also used in the $\tau^+\tau^-b\bar{b}$ analysis). The effect of this improvement is to further reduce the contribution of each single background event to the confidence level. As in Ref. [2], no background subtraction was performed. The validity of the results presented here is therefore unaffected by possible systematic uncertainties related to the knowledge of the residual background.

The final sets of selection cuts, leading to the overall smallest expected combined confidence level for $m_h = m_A = 75$ GeV/$c^2$ and $\cos^2(\beta-\alpha) = 1$, are described in the next two sections. This confidence level optimization was performed with Monte Carlo data sets corresponding to at least 100 times the integrated luminosity actually recorded for the various background processes (as described in Ref. [1]) and of 10 000 hA events generated with the `HZHA` program [20]. The result of the analysis combination when applied to the data is presented in Section 4.

## 3.1 The $b\bar{b}b\bar{b}$ final state

The signature of the $b\bar{b}b\bar{b}$ channel is a four-jet topology and a high b quark content. The three main sources of background to the four-jet topology are hadron production $e^+e^- \to q\bar{q}gg$, and ZZ and $W^+W^-$ production. The preselection of hadronic four-jet events is essentially identical to that applied to the 130–172 GeV data [2]: the Durham algorithm was used to cluster the event into four jets, and the $y_{cut}$ transition value between three and four jets was required to be greater than 0.001; events with radiative returns to the Z resonance were rejected by requiring that $|p_z| \leq 1.5(m_{vis} - 90)$, where $p_z$ and $m_{vis}$ are the total momentum along the beam direction (in GeV/$c$) and the total visible mass (in GeV/$c^2$) of the event, respectively. The only change in the preselection was that the upper cut on the thrust was relaxed from 0.85 to 0.90. This improves the signal efficiency slightly while the majority of additional background

events selected have a low dijet mass sum (below 100 GeV/$c^2$) for the dijet combination with the smallest mass difference, thus not affecting the signal search region.

The signal efficiency after this preselection is 95%, while the $q\bar{q}gg$, ZZ and $W^+W^-$ backgrounds are reduced by factors of roughly 25, 6 and 2, respectively. A total of 755 events was observed in the data, in satisfactory agreement with the 701 events expected from the simulation (218 $q\bar{q}$, 29 ZZ, and 454 $W^+W^-$). The last step combines b-tagging information and a measurement of the four-jet compatibility. The b-tagging variable $\mathcal{B}_4$ is related to the sum of the four neural network outputs $\eta_j$,

$$\mathcal{B}_4 = 4 - \sum_{j=1}^{4} \eta_j \, ,$$

and the four-jet compatibility is gauged with the smallest jet-jet angle $\theta_{ij}^{\min}$. As in Ref. [2], these two quantities are combined into a single variable

$$\mathcal{F} = 90\mathcal{B}_4 - \theta_{ij}^{\min} \quad (\theta_{ij}^{\min} \text{ in degrees}),$$

the distribution of which is shown in Fig. 1. The optimized cut value $\mathcal{F} < 67$ leads to a signal efficiency of 60.5% for $m_{\mathrm{h}} = 75$ GeV/$c^2$, corresponding to 3.10 signal events expected, while $2.4 \pm 0.1$ events are expected from the background (1.1 $q\bar{q}$, 1.0 ZZ and 0.3 $W^+W^-$ events). Two events were selected in the data.

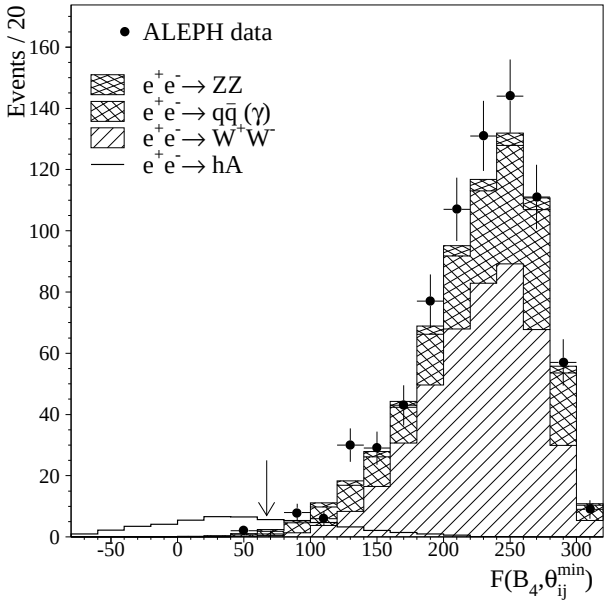


Figure 1: Distribution of the $\mathcal{F}$ variable at the preselection level of the $b\bar{b}b\bar{b}$ analysis. The expected background sources are shown in the cumulative shaded histograms while the expected signal ($m_{\mathrm{h}} \sim m_{\mathrm{A}} \sim 75$ GeV/$c^2$) is magnified ten times. The arrow shows the cut value on $\mathcal{F}$.

Systematic studies were performed to estimate the uncertainty on the signal selection efficiency. The dominant uncertainty comes from b tagging. The effect of the underlying

physics distribution was studied by varying the momenta, lifetimes and multiplicities of the b hadrons within their current experimental uncertainties using a reweighting method. Varying the b hadron lifetimes around the world average value results in a 0.7% uncertainty for the signal efficiency. The systematic error associated with varying the multiplicity and b hadron momentum spectrum within their uncertainties were estimated to be 0.4%. The efficiency uncertainty due to the simulation of the detector response was estimated as described in Ref. [2] to be approximately 2.0%. The size of the hA Monte Carlo sample gives an additional 0.5% systematic uncertainty on the efficiency. The total systematic uncertainty, taken into account in the final setting of the limit, therefore amounts to 2.2%.

## 3.2 The $\tau^+\tau^-b\bar{b}$ final state

Events in the $\tau^+\tau^-b\bar{b}$ final state are characterized by a pair of energetic and isolated narrow jets (originating from the $\tau$ decays) and a pair of energetic hadronic jets, accompanied by missing energy and transverse momentum. In place of the jet- and track-based $\tau$ identification algorithms used previously [2], a unique and simpler $\tau$ identification based upon "minijets" was developed and found to give performance similar to the combination of the former two. It is performed as follows.

The energy flow particles of the hadronic events are clustered into minijets using the invariant mass algorithm, with a mass cut of 2.7 GeV/$c^2$. Ten minijets are typically formed in a signal event. To be considered as a $\tau$ candidate, a minijet must be isolated, narrow, and energetic, according to the following criteria.

1. The minijet isolation angle, defined as the half-angle of the largest cone around the minijet direction containing less than 5% of the total energy of the other minijets in the event, must exceed 15°.

2. The minijet charged multiplicity (counted with particles of momentum in excess of 1 GeV/$c$) must be one, two or three; minijets with three charged particles are required to have unit charge, and the charge of minijets with multiplicity two is defined to be the charge of the higher momentum charged particle.

3. The energy of a minijet with two or three good tracks is required to be larger than 12.5 GeV; this cut is loosened to 7.5 GeV for a minijet with one prong if the charged particle carries less than 80% of its energy, unless it is identified as an electron or a muon in which case no such cut is applied to allow for the presence of two neutrinos from the $\tau$ decay. In contrast, in case the minijet contains an identified lepton, the energy of this lepton must be less than 25% of the centre-of-mass energy to reject WW and ZZ events with leptonic decays.

Energetic converted photons (*e.g.*, from radiative return to the Z peak) usually satisfy these three criteria. To reject these candidate $\tau$'s, it was required that *(i)* minijets consisting of a single identified electron be associated with at least one hit in the vertex detector and that this electron not form an identified $V^0$ [16] with another charged particle; and *(ii)* no electrons be identified in minijets with two charged particles. The remaining events from radiative return to

the Z resonance (with an energetic unconverted photon) were rejected by cutting on the total missing energy $E_{\rm miss}$ and the total missing longitudinal momentum $p_z$ ($|p_z| + E_{\rm miss} \leq 1.8E_{\rm peak}$ and $|p_z| \leq 0.6E_{\rm peak}$), for those events in which the photon escapes undetected along the beam direction with an expected energy $E_{\rm peak} = (s - {m_{\rm Z}}^2)/2\sqrt{s}$, and on the energy $E_\gamma$ of the most energetic photon ($E_\gamma \leq 0.6E_{\rm peak}$) for the others.

Events were selected with at least two such $\tau$ candidates of opposite electric charges, of which at least one contains exactly one charged particle. Some missing energy and momentum was ensured by requiring the total missing momentum transverse to the beam to be greater than 2.5% of the centre-of-mass energy.

The energy flow particles were then separated into the two $\tau$ minijets and the rest, clustered into two hadronic jets with the Durham algorithm. A kinematic fit was performed to determine the four jet energies, fixing the hadronic jet velocities and the $\tau$ jet directions to the measured ones, fixing the $\tau$ jet masses to $m_\tau$, constraining the invariant masses of the $\tau$ jet pair and of the hadronic jet pair to be equal, and imposing total energy-momentum conservation. The fitted hadronic jet energies were required to exceed 75% of the measured energies. Finally, if several configurations of $\tau$ candidates and hadronic jets were found to satisfy all the above requirements, only that with the smallest $\chi^2$ was kept.

This preselection preserves 57% of the signal and yields an expected background of $61.7 \pm 0.6$ events, dominated by $\rm W^+W^-$, with 56 events observed in the data. Four additional quantities were used so that $\rm hA \to b\bar{b}\tau^+\tau^-$ events (with $m_{\rm h} = m_{\rm A} = 75\ {\rm GeV}/c^2$) are further discriminated from the preselected background events:

- the total transverse momentum of the event;
- the sum of the two $\tau$ minijet isolation angles;
- the $\chi^2$ of the kinematic fit;
- the b content of the two hadronic jets ($B_2 = \eta_1 + \eta_2$).

Better performance is obtained when these four quantities are combined using a multivariate analysis. Here, a neural network technique is used. The distributions of the neural network output as expected for signal and background processes and observed in the data are shown in Fig. 2. The optimized cut value of 0.96 leads to a signal efficiency of 28.6 % for $m_{\rm h} = m_{\rm A} = 75\ {\rm GeV}/c^2$, corresponding to 0.27 signal events expected, with 0.07 background events expected.

No events were selected in the data.

The systematic uncertainties arising from b tagging were evaluated as described in the previous section. Varying the b jet multiplicity and momentum spectrum results in 0.6% and 0.2% uncertainties on the selection efficiency. The uncertainty due to the simulation of the detector response was found to be 0.5%, while that due to the b lifetime is negligible.

Additional uncertainties arise from possible discrepancies between the data and the simulation in jet reconstruction and event kinematics. To estimate these effects, jet directions and energies were smeared, the most relevant Monte Carlo distributions (total missing

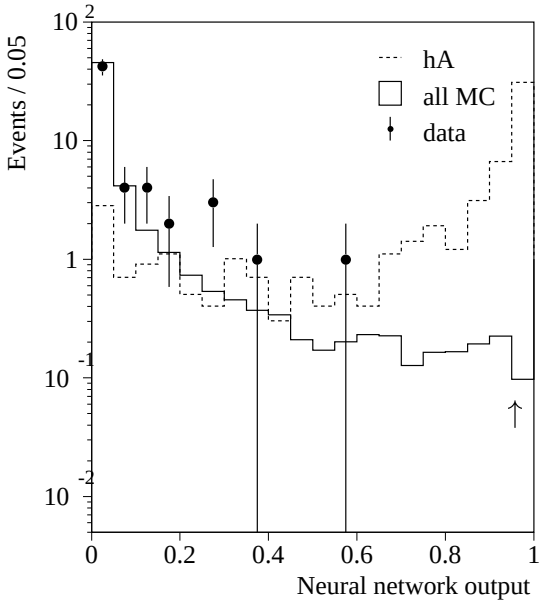


Figure 2: Neural network output distributions in the $\tau^+\tau^-\mathrm{b\bar{b}}$ analysis, as expected from background (solid curve), from signal (dashed curve, arbitrary scale), and as observed in the data (dots with error bars). The arrow shows the cut value for the neural network output.

transverse momentum, total missing energy) were reweighted to match those of the data at the preselection level, and the signal efficiency was determined again. Uncertainties in other variables were found to have a negligible impact upon the signal efficiency. As a result, a total systematic uncertainty of 0.5% was assigned to these possible effects.

The systematic uncertainty from all sources in this channel is therefore 0.9% which, when combined with the 1.5% uncertainty due to the limited number of signal Monte Carlo events, sets the total systematic uncertainty in the $\tau^+\tau^-\mathrm{b\bar{b}}$ channel to 1.8%.

# 4 Results in the benchmark cases

The searches described in the previous sections selected two events in the data with 2.5 expected from standard model background processes. The two candidate events were selected in the $\mathrm{b\bar{b}b\bar{b}}$ channel, with reconstructed $m_\mathrm{h} + m_\mathrm{A}$ values of 57.8 and 130.2 GeV/$c^2$. The confidence levels expected and observed in the two channels are displayed in Figs. 3a and b, for equal h and A masses and $\cos^2(\beta-\alpha) = 1$.

These results were combined with the lower energy results, obtained with data taken at $\sqrt{s}$ from 130 to 172 GeV, as shown in Fig. 3c. In the MSSM, for $\cos^2(\beta-\alpha) = 1$ (*i.e.*, at large $\tan\beta$), the hA selection combination excludes all h and A masses below 76.1 GeV/$c^2$ at the 95% confidence level, with an expected limit of 71.7 GeV/$c^2$. The probability to observe at least as high a limit is 23%.

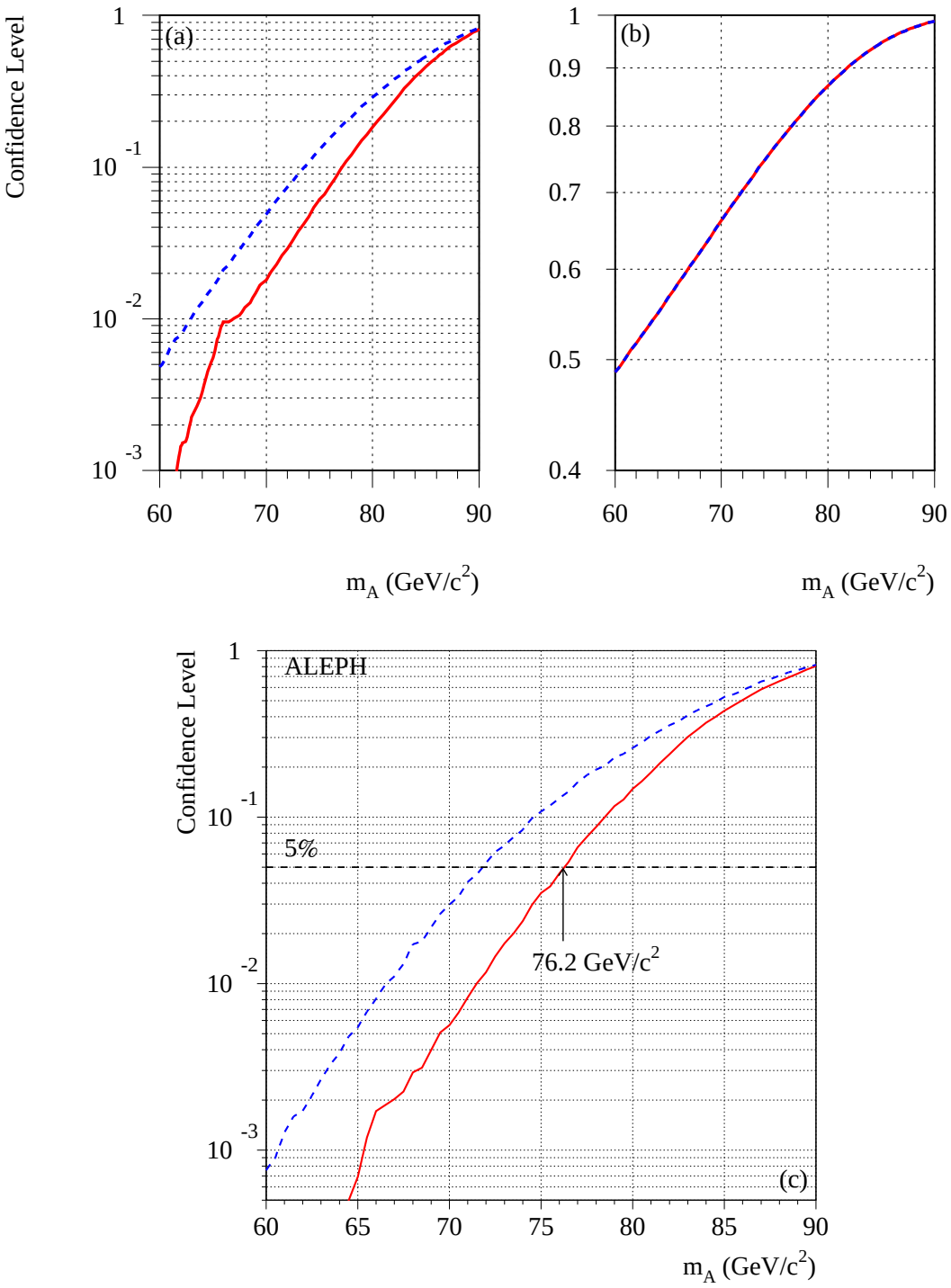


Figure 3: Confidence levels observed (solid curves) and expected (dashed curves) for the hA pair-production process with $m_{\mathrm{h}} = m_{\mathrm{A}}$ as a function of the common mass, in (a) the $\mathrm{b\bar{b}b\bar{b}}$ final state; (b) the $\tau^+\tau^-\mathrm{b\bar{b}}$ final state; and (c) combined with lower energy ALEPH results. In (b), the expected and observed confidence levels are hardly distinguishable.

The hZ [3] and hA searches can also be interpreted at lower $\cos^2(\beta-\alpha)$ values as was done in Ref. [2]. An almost parameter-independent limit (with the same caveats as in Ref. [2]) can be obtained in the [$m_{\rm h}$, $\sin^2(\beta-\alpha)$] plane, from a reinterpretation of the various selections, *(i)* for the hZ process, the cross section of which is proportional to $\sin^2(\beta-\alpha)$; and *(ii)* for hA production, with a cross section proportional to $\cos^2(\beta-\alpha)$. The results are displayed in Fig. 4, together with that of the combination of the hZ and hA results.

These results can also be expressed in the [$m_{\rm h}$,$\tan\beta$] plane, as is done in Fig. 5 for the benchmark sets of MSSM parameters [5], where $\rm M_{SUSY}$, the quadratic mean of the two stop masses, is fixed to 1 TeV/$c^2$, and for two extreme configurations of stop mixing controlled by $A_{\rm t}$ and $\mu$: minimal mixing ($A_{\rm t}, \mu \ll \rm M_{SUSY}$) and maximal mixing ($A_{\rm t} - \mu/\tan\beta = \sqrt{6}\rm M_{SUSY}$). An absolute lower limit of 72.2 GeV/$c^2$ is derived for $m_{\rm h}$, irrespective of $\tan\beta$. If $\tan\beta$ is restricted to exceed 1, this corresponds to a lower limit of 76.1 GeV/$c^2$ for $m_{\rm A}$. These values include the effect of the systematic uncertainties, taken into account following the method of Ref. [21], and resulting in a change in the mass limits of about $-20$ MeV/$c^2$.

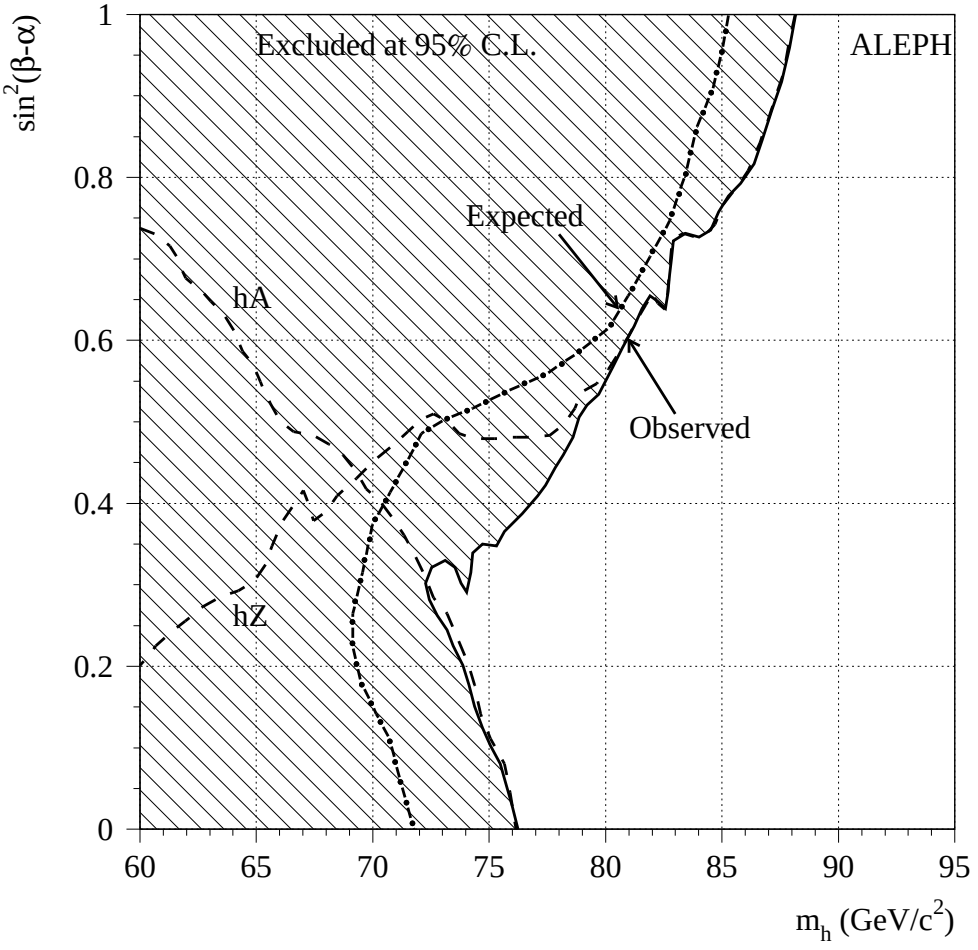


Figure 4: Regions excluded at the 95% confidence level in the [$m_{\rm h}$,$\sin^2(\beta-\alpha)$] plane by the hZ and hA searches (dashed curves) and their combination (solid curve). The dash-dotted curve displays the expected 95% C.L. limit in this plane.

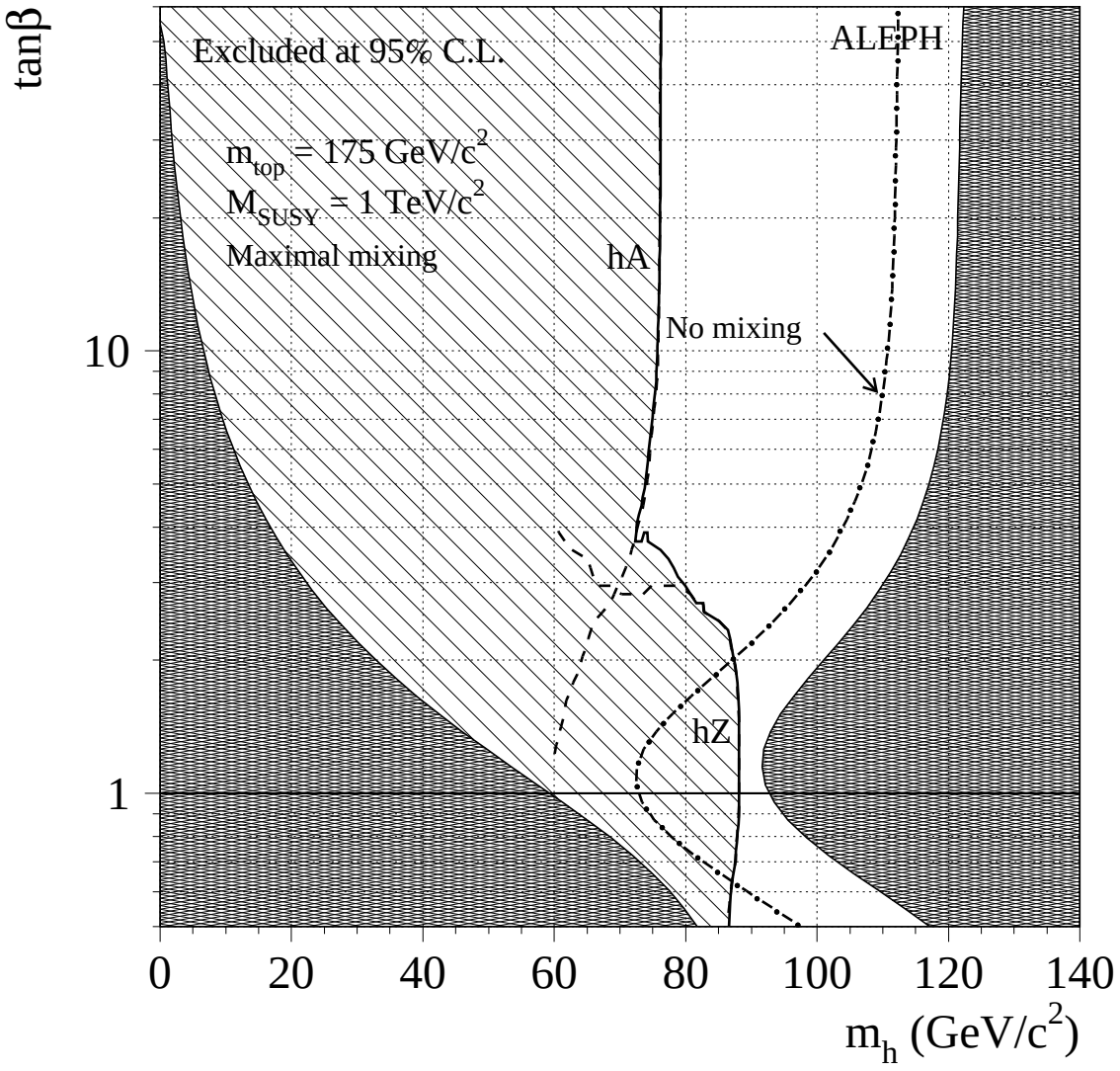


Figure 5: Regions excluded at the 95% confidence level by the hZ and hA searches (dashed curves) and their combination (solid curve), for a set of MSSM parameters corresponding to maximal stop mixing and to a SUSY mass scale of 1 TeV/$c^2$. The dark regions are not allowed theoretically. The combined experimentally excluded region is essentially identical in the case of no stop mixing, for which the theoretically forbidden region is also indicated (dash-dotted curve).

# 5 Beyond the benchmark

In this section, it is investigated how the results obtained in the benchmark cases of minimal and maximal mixing are affected when the model parameters are allowed to vary. The study is conducted within the framework of a "semi-constrained" MSSM. Universal SUSY breaking masses $m_0$ and $m_{1/2}$ are assumed for all matter scalars and for the three gauginos at the GUT scale, respectively, but no such constraint is imposed in the Higgs sector and radiative breaking of the electroweak symmetry is not enforced. Therefore, the CP-odd Higgs boson mass $m_{\rm A}$ and the Higgs mixing supersymmetric mass $\mu$ remain as free parameters. The parameter set is further specified by the values of $\tan\beta$ and of the trilinear coupling $A_{\rm t}$ which controls the stop mixing. The other trilinear couplings are assumed for simplicity to be equal to $A_{\rm t}$. (This choice has very little impact on what follows.) Once such a parameter set $\{m_0,\ m_{1/2},\ \mu,\ \tan\beta,\ A_{\rm t},\ m_{\rm A}\}$ is specified, the masses and couplings of all sleptons, squarks, gauginos and Higgs bosons can be calculated, and hence all production cross sections and decay branching ratios [20, 22].

Such an exploration of the MSSM parameter space is expected to lead to the identification of parameter sets such that

*i)* either the cross section of the Higgs-strahlung process is vanishingly small for some low $m_{\rm h}$ value, but this is not compensated by a large cross section for the pair production reaction because of too large an $m_{\rm A}$ value; such situations are anomalous in the sense that a small ZZh coupling normally goes together with h and A bosons close in mass;

*ii)* or the Higgs boson decay patterns prevent the usual Higgs boson searches from being efficient, as for instance in the case of a vanishing hbb coupling.

The study presented here is an attempt to quantify the level of fine tuning which these anomalous configurations require and, from this point of view, represents an expansion on Refs. [23] and [24]. A detailed account of this analysis can be found in Ref. [6].

## 5.1 Constraints on the parameter sets

The following theoretical and experimental constraints are used to decide whether a given parameter set is excluded or not, with $R$-parity conservation assumed throughout.

- No particles of the MSSM spectrum should be tachyonic, and the lightest supersymmetric particle must be the lightest neutralino $\chi$. This defines the physically acceptable sets.
- The masses of charginos, sleptons and stops must exceed their most recent ALEPH limits [9, 10]. The sneutrino mass must exceed its LEP1 limit of 43 GeV/$c^2$, inferred from the Z width measurement [11].
- The LEP1 limit on $\sin^2(\beta-\alpha)$ as a function of $m_{\rm h}$ must be satisfied. The published ALEPH results [13] have been updated according to Ref. [12] using the full LEP1

statistics. The resulting constraint on $\sin^2(\beta-\alpha)$ is applied, taking into account the h decay branching ratios into standard-model-like final states or into pairs of A bosons.

- The LEP1 constraints on $\cos^2(\beta-\alpha)$ as a function of $m_{\mathrm{h}}$ and $m_{\mathrm{A}}$ are enforced. First, the partial width of the $\mathrm{Z} \to \mathrm{hA}$ decay must be smaller than 7 MeV; this limit is deduced from the Z width measurement assuming a light Higgs boson. Next, the published ALEPH results [13] on searches for $\mathrm{e^+e^-} \to \mathrm{hA}$ have been updated and are used in the present analysis for $m_{\mathrm{A}} > 2m_{\mathrm{b}}$, taking into account the values of the h and A decay branching ratios into $\tau^+\tau^-$ and into hadrons. Finally, to cope with the configuration where $m_{\mathrm{A}} < 2m_{\mathrm{b}}$, in which case the $\mathrm{e^+e^-} \to \mathrm{hA}$ process leads to a three-jet topology when $\mathrm{h} \to \mathrm{AA}$, a search for final states consisting of three jets, of which one reduces to a $\mu^+\mu^-$ pair, was developed [6]. Although small, the branching ratio of $\mathrm{A} \to \mu^+\mu^-$ is never negligible when $m_{\mathrm{A}} < 2m_{\mathrm{b}}$, and the results of this simple analysis turn out to be sufficiently constraining whenever they are needed.

- The upper limit on $\sin^2(\beta-\alpha)$ as a function of $m_{\mathrm{h}}$ reported in Section 4 (Fig. 4) must be satisfied. Possible reductions of the sensitivity of the searches for $\mathrm{e^+e^-} \to \mathrm{hZ}$ due to an h decay branching ratio into $\mathrm{b\bar{b}}$ lower than in the standard model are taken into account. It has been verified that the efficiencies of the searches in the $\mathrm{h}\ell^+\ell^-$ and $\mathrm{h}\nu\bar{\nu}$ final states are unaffected if h decays to a pair of A bosons when $m_{\mathrm{A}} > 2m_{\mathrm{b}}$. In contrast, a reduction of the selection efficiency occurs in the $\mathrm{hq\bar{q}}$ channel when $\mathrm{h} \to \mathrm{AA}$, due to the six-jet rather than four-jet structure of the final state. This is taken into account when relevant. A null efficiency is assumed in the case of $\mathrm{h} \to \mathrm{AA}$ decays when $m_{\mathrm{A}} < 2m_{\mathrm{b}}$.

- For a Higgs boson decaying invisibly, the $\sin^2(\beta-\alpha)$ limit as a function of $m_{\mathrm{h}}$ is taken from Refs. [8] and [13]. Here, the value of the branching ratio of $\mathrm{h} \to \chi\chi$ is taken into account.

- The upper limit on $\cos^2(\beta-\alpha)$ as a function of $m_{\mathrm{h}}$ reported in Section 4 (Fig. 4) must be satisfied. The values of the h and A decay branching ratios into $\tau^+\tau^-$ and into $\mathrm{b\bar{b}}$ are taken into account. The efficiency reduction which takes place in the case of unequal masses has been mapped as a function of $m_{\mathrm{h}}$ and $m_{\mathrm{A}}$ [6].

- The mass of the charged Higgs boson must exceed its lower limit as a function of its decay branching ratio into $\tau\nu$, as determined by ALEPH searches [7] for $\mathrm{e^+e^-} \to \mathrm{H^+H^-}$.

In addition, it occasionally happens that valuable constraints are obtained by the replacement of h by H, where H is the heavier CP-even neutral Higgs boson, with the appropriate coupling modifications.

Ultra-light Higgs bosons, *i.e.*, $m_{\mathrm{h}}$ or $m_{\mathrm{A}} < 2m_{\mu}$, are not considered in the present analysis. In such a case, the only allowed Higgs boson decay modes are into $\mathrm{e^+e^-}$ or $\gamma\gamma$, and the nonzero lifetimes must be explicitly taken into account. A dedicated search was performed by ALEPH [25] using LEP1 data collected until the end of 1991. The conclusion, namely that such a possibility is excluded within the benchmark case of minimal mixing, relied on a delicate combination of a large variety of signatures. Assessing how general this conclusion is would necessitate a thorough investigation which is beyond the scope of the present study.

## 5.2 Scans of the MSSM parameter space: procedure

In the scans described below, a top quark mass of 175 GeV/$c^2$ is assumed unless otherwise specified. Nine values of $\tan\beta$ were probed, $\{1/\sqrt{2},\ 1,\ \sqrt{2},\ 2,\ 2\sqrt{2},\ 4,\ 8,\ 16,\ 32\}$. Various samplings, summarized in Table 1, were used for the dimensionful parameters $m_0$, $m_{1/2}$, $|\mu|$ and $|A_t|$, with both signs for $\mu$ and $A_t$: *i)* nine values for the "coarse logarithmic" scans, $\{0$ and $2000/2^n\}$ GeV/$c^2$ with $n = 7$ to 0, supplemented with a tenth value for $|A_t|$, 4000 GeV/$c^2$; *ii)* seventeen values for the "fine logarithmic" scans, $\{0$ and $2000/2^{n/2}\}$ GeV/$c^2$ with $n = 15$ to 0, supplemented with two more values for $|A_t|$, $2000\sqrt{2}$ and 4000 GeV/$c^2$; *iii)* eleven values for the "linear" scans, $\{0$ and $200n\}$ GeV/$c^2$ with $n = 1$ to 10, supplemented with two more values for $|A_t|$, 2200 and 2400 GeV/$c^2$.

Table 1: Summary of the definition of the scan procedures for $m_0$, $m_{1/2}$, $|\mu|$, and $|A_t|$. For a given parameter, $N_{\text{values}}$ is the number of values considered in the scan.

| Scan | Values (GeV/$c^2$) | Parameters | | | |
|---|---|---|---|---|---|
| | | $m_0$, $m_{1/2}$, $\lvert\mu\rvert$ | | $\lvert A_t\rvert$ | |
| | | $n$ range | $N_{\text{values}}$ | $n$ range | $N_{\text{values}}$ |
| Coarse logarithmic | $\{0,\ 2000/2^n\}$ | $n$: $7 \to 0$ | 9 | $n$: $7 \to -1$ | 10 |
| Fine logarithmic | $\{0,\ 2000/2^{n/2}\}$ | $n$: $15 \to 0$ | 17 | $n$: $15 \to -2$ | 19 |
| Linear | $\{0,\ 200 \times n\}$ | $n$: $1 \to 10$ | 11 | $n$: $1 \to 12$ | 13 |

Coarse logarithmic scans were performed for the nine selected values of $\tan\beta$. Moreover, for two values of $\tan\beta$, namely $\sqrt{2}$ and 32, which are typical of the low and high $\tan\beta$ regimes, fine logarithmic scans were also performed. Finally, for those two same $\tan\beta$ values, additional scans were made: linear scans in order to investigate possible dependences of the results on the way the parameter space is sampled; and coarse logarithmic scans for $m_t = 170$ and 180 GeV/$c^2$ to study the sensitivity of the results to the top quark mass. In the coarse logarithmic scans, 26 163 sets of $\{m_0,\ m_{1/2},\ \mu,\ A_t\}$ values are explored, 352 869 sets in the fine logarithmic scans and 63 525 in the linear scans.

For each of those $\{\tan\beta,\ m_0,\ m_{1/2},\ \mu,\ A_t\}$ sets, the lower limit on $m_h$ is determined in the following way. First, $m_A$ is incremented using a still finer logarithmic sampling consisting of 35 values, $\{0$ and $2000/2^{n/4}\}$ GeV/$c^2$ with $n = 33$ to 0. The $m_A$ scan is interrupted as soon as a value leading to an unexcluded situation is encountered, according to the criteria listed in the previous subsection. The interval separating the last excluded value and the first unexcluded value is then explored using a dichotomy technique to find the value of the limit on $m_h$. Explorations are also performed between successive values of $m_A$ which are not excluded by at least one common constraint, or for which opposite signs of $\sin(\beta-\alpha)$, $\cos(\beta-\alpha)$, or $\sin\alpha$ are encountered. (In such cases, the $e^+e^- \to hZ$ cross section, the $e^+e^- \to hA$ cross section, or the $h \to b\bar{b}$ branching ratio, respectively, is expected to vanish somewhere in between.)

Altogether, the nine coarse logarithmic scans represent a sampling of the parameter space consisting of 8.2 million sets of $\{\tan\beta,\ m_0,\ m_{1/2},\ \mu,\ A_t,\ m_A\}$ values, and the two fine logarithmic

scans each represent a sampling of 12.4 million sets of $\{m_0,\ m_{1/2},\ \mu,\ A_t,\ m_A\}$ values, not including the additional $m_A$ values tested in the dichotomy procedures.

## 5.3 Scans of the MSSM parameter space: results

The low $\tan\beta$ regime is specifically addressed by the fine logarithmic scan for $\tan\beta = \sqrt{2}$. Out of the 352 869 sets of $\{m_0,\ m_{1/2},\ \mu,\ A_t\}$ values explored, 127 994 are unphysical and 142 204 are rejected by the constraints on supersymmetric particles. Out of the 82 671 remaining sets, 41 319 are excluded irrespective of the value of $m_A$, which means that $\tan\beta = \sqrt{2}$ is excluded for such sets. The benchmark case with minimal mixing is an example of such a configuration (Fig. 5). The distribution of the $m_h$ limit for the 41 352 other sets is shown in Fig. 6a. In the vast majority of cases, the limit is indistinguishable from that obtained in the case of maximal mixing from the search for the Higgs-strahlung process at LEP2 (Fig. 5), *i.e.*, 88 GeV/$c^2$. The limit is nevertheless significantly lower for 28 sets, which is to be compared to a total of about 225 000 physically acceptable sets. The proportion of sets for which the $m_h$ limit is degraded is therefore at the $10^{-4}$ level. These "pathological" sets correspond to the anomalous configurations which had been anticipated, namely a vanishing ZZh or $\mathrm{hb\bar{b}}$ coupling.

The additional scans for $\tan\beta = \sqrt{2}$ do not reveal any new anomalous features. The linear scan leads to a similar fraction of pathological sets. The only noticeable effect of increasing (decreasing) the top quark mass is to reduce (increase) the fraction of sets excluded irrespective of the value of $m_A$, but the proportion of sets leading to a significantly reduced $m_h$ limit is unaffected.

Similar investigations have been made for the high $\tan\beta$ regime. In the fine logarithmic scan for $\tan\beta = 32$, out of the 352 869 sets explored 120 223 are unphysical and 150 647 are rejected by the constraints on supersymmetric particles. Out of the 81 999 remaining sets, only 434 are excluded irrespective of the value of $m_A$, which is not unexpected for such a large value of $\tan\beta$ (Fig. 5). The distribution of the $m_h$ limit for the 81 565 other sets is shown in Fig. 6b. While a peak is clearly visible at 76 GeV/$c^2$, *i.e.*, the value obtained for maximal mixing, a broad tail is seen to extend to lower masses. (For instance, a total of 1 572 sets is found to lead to a limit smaller than the benchmark absolute limit of 72 GeV/$c^2$.) This comes from the fact that the main rôle is played in this high $\tan\beta$ regime by the search for $\mathrm{e^+e^-} \to \mathrm{hA}$ at LEP2, a search in which the kinematically relevant variable is $m_h + m_A$ rather than $m_h$. Indeed, it can be seen in Fig. 6c that the peak in the limit, at 152 GeV/$c^2$, is much sharper when displayed using that variable. There remain 182 sets for which a limit on $m_h + m_A$ lower than 144 GeV/$c^2$ is obtained, a fraction at the $10^{-3}$ level with respect to the number of physically acceptable sets. The characteristics of those pathological sets and the conclusions drawn from the additional scans are the same as for $\tan\beta = \sqrt{2}$.

For the nine selected $\tan\beta$ values, a summary of the results of the coarse logarithmic scans is displayed in Table 2. It can be seen that the behaviour observed for $\tan\beta = 1$ or 2 is very similar to that detailed for $\tan\beta = \sqrt{2}$, and similarly for $\tan\beta = 8$ and 16 compared to $\tan\beta = 32$. The values $\tan\beta = 2\sqrt{2}$ and 4 correspond to the transition from the low to the high $\tan\beta$ regimes and share features of both.

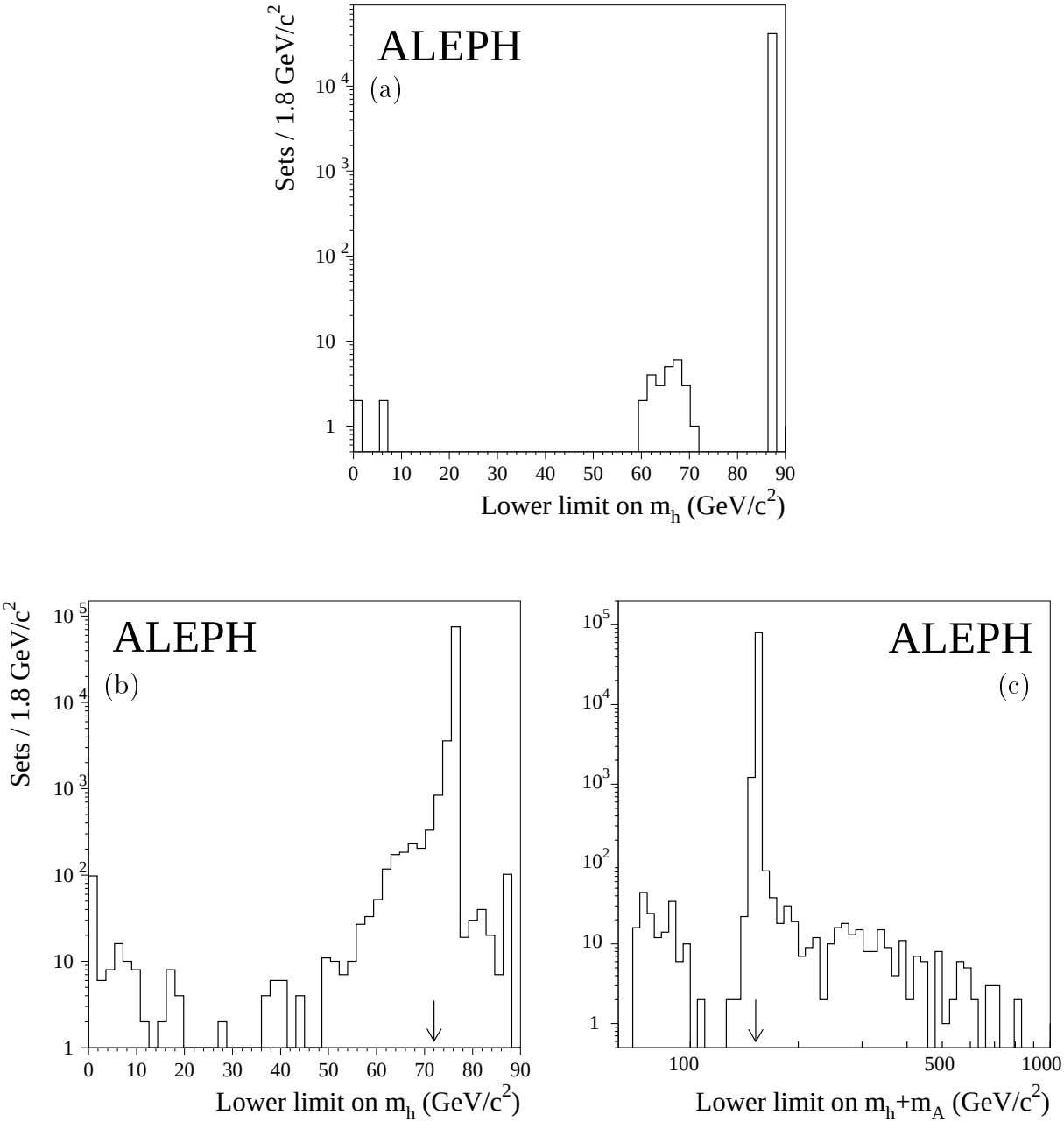


Figure 6: Distribution of the lower limit on $m_{\mathrm{h}}$, (a) for $\tan\beta = \sqrt{2}$ and (b) for $\tan\beta = 32$. (c) Distribution of the lower limit on $m_{\mathrm{h}} + m_{\mathrm{A}}$ for $\tan\beta = 32$. In (b) and (c), the arrows indicate the value of the reference mass value close to the limit obtained in the benchmark case. This value cannot be distinguished from the peak at 87 GeV/$c^2$ in (a).

Table 2: Results of the coarse logarithmic scans. The value of $\tan\beta$ is given in the first column. The second column indicates as "test" a mass value in GeV/$c^2$ close to the limit obtained in the benchmark case of "maximal mixing" either for $m_{\rm h}$ (values without asterisks) or for $m_{\rm h} + m_{\rm A}$ (values with asterisks). The third column contains the number of physically acceptable parameter sets, out of a total of 26 163 explored. The number of sets excluded by the searches for supersymmetric particles is given in the fourth column. The fifth column contains the number of sets for which the whole physical domain is excluded by the searches for Higgs bosons. The number of sets for which the limit obtained for $m_{\rm h}$ or for $m_{\rm h} + m_{\rm A}$, as relevant, is equal to (or larger than) the test value is shown in the sixth column. The number of sets for which the limit is degraded with respect to the test value is indicated in the last column. For $\tan\beta = 1/\sqrt{2}$, the first (second) line is obtained when the constraints on the charged Higgs boson mass obtained at the Tevatron [26] are not (are) taken into account.

| $\tan\beta$ | Test value (GeV/$c^2$) | Physical sets | Excluded by SUSY | Excluded by Higgs | Better limit | Worse limit |
|---|---|---|---|---|---|---|
| $1/\sqrt{2}$ | 87 | 15096 | 9666 | 168 | 691 | 4571 |
| | | | | 630 | 4788 | 12 |
| 1 | 87 | 16057 | 10106 | 3065 | 2882 | 4 |
| $\sqrt{2}$ | 87 | 16044 | 9974 | 2494 | 3570 | 6 |
| 2 | 87 | 16131 | 9971 | 1030 | 5117 | 13 |
| $2\sqrt{2}$ | 80 | 17123 | 10780 | 137 | 5923 | 283 |
| | 140 * | | | | 6204 | 2 |
| 4 | 67 | 17258 | 10797 | 45 | 6221 | 195 |
| | 140 * | | | | 6376 | 40 |
| 8 | 140 * | 17016 | 10584 | 29 | 6367 | 36 |
| 16 | 142 * | 17002 | 10570 | 20 | 6402 | 10 |
| 32 | 144 * | 16711 | 10287 | 23 | 6395 | 6 |

The case of $\tan\beta = 1/\sqrt{2}$ is quite different. The lower edge of the physical domain for $m_{\rm h}$, around 70 GeV/$c^2$, tends to be unexcluded because the search for the Higgs-strahlung process at LEP2, which involves b tagging, becomes inefficient in this configuration where $\rm h \to AA$ is dominant while $m_{\rm A} < 2m_{\rm b}$. (This problem does not arise for $\tan\beta > 1$ because such low $m_{\rm A}$ values are always associated with $m_{\rm h}$ values small enough to be well within the reach of searches at LEP1 which do not require b tagging.) It may be noticed however that the low $m_{\rm A}$ region also corresponds to rather low charged Higgs boson masses which, for $\tan\beta < 1$, have been excluded at the Tevatron [26]. Taking this additional constraint into account brings the fraction of sets for which the $m_{\rm h}$ limit is degraded in line with that found for $1 \leq \tan\beta \lesssim 2$.

In the course of the above scans, parameter sets were identified with values of $m_{\rm h}$ well below the limit obtained in the benchmark case, and such that no exclusion can ever be expected at LEP [6]. For such sets, the ZZh coupling vanishes while $m_{\rm h} + m_{\rm A}$ exceeds the ultimate kinematic reach of LEP2; moreover, the $\rm e^+e^- \to HZ$ or $\rm H^+H^-$ processes also remain kinematically unaccessible, and similarly for the production of supersymmetric particles. No qualitative changes with respect to the conclusions drawn from the present study are therefore to be expected from further LEP energy increases nor from additional integrated luminosity.

### 5.4 Results in a less constrained MSSM

The version of the MSSM used in the analysis presented above may be viewed as too restrictive, in particular because of the assumption of a universal scalar mass for all sleptons and squarks at the GUT scale. To assess the impact of this assumption, coarse logarithmic scans have been repeated for $\tan\beta = \sqrt{2}$ and 32, *(i)* ignoring all the constraints on sleptons and sneutrinos (except for the model-independent limits coming from the Z width measurement), thus allowing in particular the LSP to be a sneutrino, and *(ii)* replacing the LEP2 limits on charginos, which depend on the sneutrino mass, by the constraint $m_{\chi^\pm} > 75$ GeV/$c^2$, valid except in the case of chargino-sneutrino mass degeneracy [9]. In these scans, the $m_0$ parameter was furthermore replaced by two independent soft supersymmetry breaking masses, $m_{\rm Q}$ and $m_{\rm U}$, appearing in the diagonal terms of the stop mass matrix. This leads to a total of 235 467 sets of $\{m_{\rm Q}, m_{\rm U}, m_{1/2}, \mu, A_{\rm t}\}$ values explored for each of the two $\tan\beta$ values. The fraction of sets with a limit significantly degraded compared to the benchmark case remains at or below the $10^{-3}$ level. Similar results are obtained with linear scans. The basic conclusions of this analysis therefore do not depend on the universality assumption for squark and slepton masses.

## 6 Conclusion

Searches for neutral Higgs bosons produced in pairs through the $\mathrm{e^+e^-} \to \mathrm{hA}$ process have been carried out in the $\mathrm{b\bar{b}b\bar{b}}$ and $\tau^+\tau^-\mathrm{b\bar{b}}$ final states using the 57 pb$^{-1}$ of data collected at centre-of-mass energies from 181 to 184 GeV. The two selected candidate events are consistent with coming from standard background processes. When combined with previous ALEPH searches for neutral Higgs bosons, these observations yield 95% C.L. exclusion limits of 72.2 and 76.1 GeV/$c^2$ for $m_{\rm h}$ and $m_{\rm A}$, for standard choices of MSSM parameter sets, irrespective of $\tan\beta$.

A full scan of the MSSM parameter space revealed that the lower limit on the mass of the CP-even neutral Higgs boson is robust in the low $\tan\beta$ regime, *i.e.*, for $1 < \tan\beta \lesssim 2$: irrespective of whether the MSSM parameter space is sampled logarithmically or linearly, and at least for values of the dimensionful parameters not exceeding 2 TeV/$c^2$, the fraction of physically allowed parameter sets for which the limit on $m_{\rm h}$ of $\sim$88 GeV/$c^2$ obtained in the benchmark case is significantly reduced is at the per mil level. For larger $\tan\beta$ values, a similar conclusion holds in terms of a limit of 140–150 GeV/$c^2$ on $m_{\rm h} + m_{\rm A}$.

## Acknowledgements

We wish to congratulate our colleagues from the accelerator divisions for the very successful operation of LEP at high energy. We are indebted to the engineers and technicians in all our institutions for their contribution to the excellent performance of ALEPH. Those of us from nonmember countries thank CERN for its hospitality.

# References


[1] The ALEPH Coll., *"Search for the standard model Higgs boson in $e^+e^-$ collisions at $\sqrt{s}$ = 161, 170 and 172 GeV"*, *Phys. Lett.* **B412** (1997) 155.

[2] The ALEPH Coll., *"Search for the neutral Higgs bosons of the MSSM in $e^+e^-$ collisions at $\sqrt{s}$ from 130 to 172 GeV"*, *Phys. Lett.* **B412** (1997) 173.

[3] The ALEPH Coll., *"Preliminary Limits from Searches for Neutral Higgs Bosons in $e^+e^-$ Collisions at Centre-of-mass Energies of 181–184 GeV"*, `ALEPH 98-029, CONF 98-017`, contribution #896 to the ICHEP, Vancouver, July 1998;
The ALEPH Coll., *"Search for the standard model Higgs boson in $e^+e^-$ collisions at $\sqrt{s}$ = 181 to 184 GeV"*, CERN-EP/98-144, to appear in *Phys. Lett.* **B**.

[4] The DELPHI Coll., *"Search for neutral and charged Higgs bosons in $e^+e^-$ collisions at $\sqrt{s}$ = 161 and 172 GeV"*, *Eur. Phys. J.* **C2** (1998) 1;
The L3 Coll., *"Search for the Standard Model Higgs Boson in $e^+e^-$ Interactions at $\sqrt{s}$ = 183 GeV"*, CERN-EP/98-052, to be published in *Phys. Lett.* **B**; *"Search for Neutral Higgs Bosons of the Minimal Supersymmetric Standard Model in $e^+e^-$ Interactions at $\sqrt{s}$ = 130-183 GeV*, CERN-EP/98-072, to be published in *Phys. Lett.* **B**;
The OPAL Coll. *"Search for the standard model Higgs boson in $e^+e^-$ collisions at $\sqrt{s}$ = 161-172 GeV" Eur. Phys. J.* **C1** (1998) 425; *"A Search for Neutral Higgs Bosons in the MSSM and Models with Two Scalar Field Doublets"*, CERN-EP/98-029, to be published in *Eur. Phys. J.* **C**.

[5] M. Carena and P. Zerwas (Conveners) et al., *"Higgs Physics"*, in Physics at LEP 2, Ed. G. Altarelli, T. Sjöstrand, and F. Zwirner, CERN 96-01 (1996) 351.

[6] The ALEPH Coll., *"Higgs limits in the MSSM: Beyond the benchmark"*, `ALEPH 98-039, CONF 98-018`, contribution #897 to the ICHEP, Vancouver, July 1998.

[7] The ALEPH Coll., *"Search for charged Higgs bosons in $e^+e^-$ collisions at centre-of-mass energies from 130 to 172 GeV"*, *Phys. Lett.* **B418** (1998) 419.

[8] The ALEPH Coll., *"Search for invisible decays of the Higgs boson in $e^+e^-$ collisions"*, contribution #617 to the IECHEP, Jerusalem, August 1997.

[9] The ALEPH Coll., *"Search for charginos and neutralinos in $e^+e^-$ collisions at $\sqrt{s} \sim$ 183 GeV and the limit on the lightest neutralino"*, `ALEPH 98-071, CONF 98-040`, contribution #952 to the ICHEP, Vancouver, July 1998;
The ALEPH Coll., *"Searches for Charginos and Neutralinos in $e^+e^-$ Collisions at $\sqrt{s}$ = 161 and 172 GeV"*, *Eur. Phys. J.* **C2** (1998) 3417.

[10] The ALEPH Coll., *"Search for sleptons in $e^+e^-$ collisions at centre-of-mass energies up to 184 GeV"*, CERN EP/98-077, to be published in *Phys. Lett.* **B**;
The ALEPH Coll., *"Scalar quark searches at $\sqrt{s}$ = 181-184 GeV in $e^+e^-$ collisions"*, CERN EP/98-076, to be published in *Phys. Lett.* **B**.

[11] The LEP Collaborations ALEPH, DELPHI, L3, OPAL, the LEP Electroweak Working Group and the SLD Heavy Flavour Group, *"A Combination of Preliminary Electroweak Measurements and Constraints on the Standard Model"*, CERN-PPE/97-154.

[12] The ALEPH Coll., *"Search for the Standard Model Higgs boson with the full LEP 1 ALEPH data sample"*, *Phys. Lett.* **B384** (1996) 427.

[13] The ALEPH Coll., *"Search for a non-minimal Higgs boson produced in the reaction* $e^+ e^- \to hZ$*"*, *Phys. Lett.* **B313** (1993) 312.

[14] The ALEPH Coll., *"ALEPH: A detector for electron-positron annihilations at LEP"*, *Nucl. Instrum. Methods* **A294** (1990) 121.

[15] D. Creanza et al., *"Construction and performance of the new ALEPH vertex detector"*, Proc. of the 5th International Conference on Advanced Technology and Particle Physics, Como, Italy, October 1996.

[16] The ALEPH Coll., *"Performance of the ALEPH detector at LEP"*, *Nucl. Instrum. Methods* **A360** (1995) 481.

[17] The ALEPH Coll., *"A precise measurement of* $\Gamma(Z \to b\bar{b})/\Gamma(Z \to$ hadrons$)$*"*, *Phys. Lett.* **B313** (1993) 535.

[18] The ALEPH Coll., *"An investigation of* $\mathrm{B}^0_\mathrm{d}$ *and* $\mathrm{B}^0_\mathrm{s}$ *oscillations"*, *Phys. Lett.* **B322** (1994) 441.

[19] P. Janot and F. Le Diberder, *"Optimally combined confidence limits"*, *Nucl. Instrum. Methods* **A411** (1998) 449.

[20] P. Janot, *"The* `HZHA` *generator"*, in G. Altarelli, T. Sjöstrand, F. Zwirner (Editors), Physics at LEP 2, CERN 96-01, 1996, Vol. 2, p. 309.

[21] R.D. Cousins and V.L. Highland, *Nucl. Instrum. Methods* **A320** (1992) 331.

[22] S. Katsanevas and M. Melachroinos, *"The* `SUSYGEN` *program"*, in G. Altarelli, T. Sjöstrand, F. Zwirner (Editors), Physics at LEP 2, CERN 96-01, 1996, Vol. 2.

[23] The OPAL Coll., *"A Search for Neutral Higgs Bosons in the MSSM and Models with Two Scalar Field Doublets"*, CERN-EP/98-029.

[24] J. Rosiek and A. Sopczak, *Phys. Lett.* **B341** (1995) 419.

[25] The ALEPH Coll., *"Search for a very light CP-odd neutral Higgs boson of the MSSM"*, *Phys. Lett.* **B285** (1992) 309.

[26] P. Janot, *"Searches for new particles at present colliders"*, invited review talk presented at the IECHEP, Jerusalem, August 1997, to appear in the proceedings;
R. E. Hughes, *"Top production and decay at the Tevatron"*, contribution to the XXXIIInd Rencontres de Moriond, Electroweak Interactions and Unified Theories, March 14-21, 1998, Les Arcs, France, to appear in the proceedings.